Title
Dual effects of erastin on aggressive osteosarcoma cells: ferroptosis sensitization and anti-ferroptotic gene activation

Journal
Cytotechnology, 77(4)

ISSN
0920-9069

Authors
Burns, Gordon Daniel
Schneider, Kevin
Atilano, Shari
et al.

Publication Date
2025-08-01

DOI
10.1007/s10616-025-00795-7

ARTICLE

Dual effects of erastin on aggressive osteosarcoma cells: ferroptosis sensitization and anti-ferroptotic gene activation

Gordon Daniel Burns[1] · Kevin Schneider[1] · Shari Atilano[1] · Marilyn Chwa[1] · Steven Chang[1] · M. Cristina Kenney[1,2] · Mithalesh Kumar Singh[1,3]

Received: 22 February 2025 / Accepted: 12 June 2025 / Published online: 23 June 2025

Abstract
Osteosarcoma (OS) is a rare cancer, yet the most prevalent primary bone cancer in adolescents and young adults OS can be fatal and detrimental due to its high aggressiveness, early metastases, and chemo-resistance. Recent research suggests that drugs that induce ferroptosis could treat osteosarcoma. It is unknown how erastin-induced ferroptosis influences differential gene expression of System Xc, iron absorption, heme synthesis, and mono- (MUFA) and polyunsaturated (PUFA) fatty acid levels in aggressive OS cells. In this study, we show that erastin-induced ferroptosis decreases OS cell growth and survival by raising total ROS, mitochondrial membrane potential, and downregulating *VDAC2*. Furthermore, erastin induces elevated levels of *SLC7A11* and *SLC3A2*, but downregulation of *TFRC* and *HMOX1* in OS cells. Notably, the addition of Ferrostatin-1 protects against Erastin-induced cytotoxicity, implying that these agents induce ferroptosis. We also showed that Ferrostatin-1 provides partial protection against Erastin-induced ferroptosis by stimulating the unique transcriptional gene profile of System Xc-, MUFA, and PUFA while inhibiting iron uptake and heme production in OS cells. These findings show that Erastin inhibits the survival of aggressive OS cells, but it also increases the expression of genes linked with anti-ferroptosis activity, which could lead to preventing ferroptosis in the aggressive OS phenotype. Targeting this anti-ferroptotic differential gene expression mediated by erastin-induced ferroptosis in OS cells may help to improve erastin's efficacy.

Keywords Osteosarcoma · Ferroptosis · Erastin · Ferrosatatin-1 · ROS

Introduction

Osteosarcoma (OS) is a malignant tumor originating from primitive mesenchymal cells of the musculoskeletal system. It predominantly affects children and adolescents, accounting for approximately 2.4% of all cancers diagnosed in this age group worldwide (Lei et al. 2020; Sadykova et al. 2020). Due to its aggressive nature and propensity for developing resistance to treatment, OS is associated with high rates of morbidity and mortality, contributing to an overall poor prognosis (Zhang et al. 2018). In the United States, approximately 400 new cases are diagnosed annually in children and young adults (Mirabello et al. 2009; Ottaviani and Jaffe 2009).

Deceased: M. Cristina Kenney

Current standard treatment, comprising surgical resection combined with multi-agent chemotherapy typically doxorubicin and cisplatin, with or without methotrexate achieves long-term survival in approximately 70% of patients (Sadykova et al. 2020; Mirabello et al. 2009; Ottaviani and Jaffe 2009). Response to preoperative combination chemotherapy remains the most reliable prognostic indicator for overall survival in patients with localized OS (Collins et al. 2013). However, outcomes for patients with metastatic or relapsed disease have seen little improvement over the past three decades, with 5-year survival rates remaining at approximately 20% (Bernthal et al. 2012; Meyers et al. 2011). Although targeted therapies and immunotherapy have advanced treatment for some malignancies, their impact on OS has been limited. Resistance to therapy and disease recurrence continue to pose significant challenges, underscoring the urgent need for more effective therapeutic strategies.

Ferroptosis is an iron-dependent form of regulated cell death driven by the accumulation of lipid hydroperoxides (LOOH) and has been implicated in the suppression of cancer cell proliferation (Wang 2020; Zilka et al. 2017). Therapeutic induction of ferroptosis has shown promising anti-tumor activity in musculoskeletal malignancies, including OS (Brack et al. 2020; Torii et al. 2016). Deeper understanding of the molecular mechanisms regulating ferroptosis is essential for advancing treatment strategies. Current therapies predominantly trigger apoptosis; however, apoptotic resistance remains a major limitation and contributes to poor clinical outcomes (Xu et al. 2019). While modest increases in reactive oxygen species (ROS) may enhance tumor progression, excessive ROS can induce irreversible oxidative damage, ultimately activating ferroptotic cell death.(Galadari et al. 2017; Hedrick et al. 2019).

Glutathione peroxidase 4 (GPX4), a glutathione (GSH)-dependent enzyme, plays a pivotal role in cellular antioxidant defense by directly reducing lipid hydroperoxides (LOOH) to their corresponding non-toxic lipid alcohols. This unique function enables GPX4 to inhibit lipid peroxidation and prevent ferroptosis, a form of regulated cell death driven by oxidative stress (Yang et al. 2014; Ursini et al. 2022; Zhang et al. 2024). Ferroptosis inducers such as RSL3 and erastin have demonstrated therapeutic potential in musculoskeletal cancer models (Codenotti et al. 2018; Schott et al. 2015). Erastin activates the ferroptotic pathway by binding to voltage-dependent anion channels (VDAC), thereby disrupting mitochondrial function (Yang et al. 2020). In combination with pharmacological agents such as celastrol, erastin enhances reactive oxygen species (ROS) production, leading to mitochondrial membrane depolarization, degradation, and fission (Liu et al. 2021). Ferrostatin-1, a ferroptosis inhibitor, prevents lipid hydroperoxide (LOOH) accumulation and may attenuate the cytotoxic effects of erastin (Yang et al. 2020).

Therefore, the primary objective of this study was to elucidate the molecular mechanisms by which erastin induces ferroptosis in OS cells, with a specific focus on the regulation of System Xc^-, enzymes of lipid metabolic pathways, and iron-homeostasis genes. By characterizing these responses and examining how they are modulated by the ferroptosis inhibitor ferrostatin-1 (Fer-1), we aim to identify transcriptional signatures associated with ferroptotic vulnerability and potential therapeutic targets for advanced OS.

Material and methods

Cell culture

The 143B OS cell line was obtained from the American Type Culture Collection (ATCC). Cells were cultured in Minimum Essential Medium (MEM; Biochrom, Berlin, Germany) supplemented with 10% fetal bovine serum (FBS), 10% dialysed FBS, 10 mM L-glutamine, 100 U/mL penicillin, 100 µg/mL streptomycin, and 2.5 µg/mL fungizone. Cultures were maintained at 37 °C in a humidified incubator under normoxic conditions (5% CO_2). Routine screening for mycoplasma contamination was performed using the Universal Mycoplasma PCR Detection Kit (ATCC).

Reconstitution of erastin and ferrostatin-1 (Fer-1)

Erastin (Cat. # S7242, Selleckchem, PA, USA) and ferrostatin-1 (Fer-1) were initially dissolved in DMSO to prepare stock solutions and subsequently diluted in culture medium to final working concentrations of 2.25 µM for erastin and 2 µM for Fer-1. These concentrations were used consistently across all experimental conditions.

MTT assay

143B cells were seeded at a density of 10,000 cells per well in flat-bottomed 96-well plates and incubated at 37 °C for 24 h. Cells were then subjected to one of four treatment conditions for the following 48 h: DMSO vehicle control; erastin administered during the final 24 h; continuous treatment with ferrostatin-1 (Fer-1) for 48 h; or pre-treatment with Fer-1 for 24 h followed by combined treatment with erastin and Fer-1 for an additional 24 h. Cell metabolic activity was assessed using the MTT assay (Cat. #30,006, Biotium, CA, USA). MTT reagent was added to the cultures and incubated for 2 h. Absorbance was measured at 570 nm with a reference wavelength of 630 nm using an ELx808 spectrophotometer (BioTek, Winooski, VT, USA). Background absorbance was subtracted, and all values were normalized to the DMSO-treated control group. Each condition was tested in six technical replicates, and the experiment was independently repeated three times.

Reactive oxygen species (ROS) assay

A total of 10,000 143B cells were seeded per well in a flat-bottomed 96-well plate and incubated at 37 °C for 24 h. Cells were then assigned to one of four treatment groups for the subsequent 48 h: a DMSO vehicle control; erastin treatment during the final 24 h; ferrostatin-1 (Fer-1) treatment for the full 48 h; or pre-treatment with Fer-1 for 24 h followed by co-treatment with Fer-1 and erastin for the remaining 24 h. Intracellular reactive oxygen species (ROS) levels were quantified using the fluorescent probe 2′,7′-dichlorodihydrofluorescein diacetate (H_2DCFDA; Invitrogen-Molecular Probes, Carlsbad, CA, USA). Fluorescence was measured using a Gemini XPS microplate reader (Molecular Devices, Sunnyvale, CA, USA) at an excitation wavelength of 490 nm and an emission wavelength of 520 nm. Fluorescence values were normalized to both the DMSO vehicle control and to cell viability to account for differences in cell numbers. Each treatment was performed in six technical replicates, and the experiment was independently repeated three times.

Mitochondrial membrane potential (JC1) assay

143B cells (10,000 cells/well) were seeded in flat-bottomed 96-well plates and incubated at 37 °C for 24 h. Cells were then treated under the following conditions for a total of 48 h: DMSO vehicle control; erastin added during the final 24 h; continuous treatment with ferrostatin-1 (Fer-1) for 48 h; or pre-treatment with Fer-1 for 24 h followed by co-treatment with both erastin and Fer-1 for the subsequent 24 h. Mitochondrial membrane potential ($\Delta\Psi$m) was assessed using the JC-1 dye (5,5′,6,6′-tetrachloro-1,1′,3,3′-tetraethylbenzimidazolylcarbocyanine iodide; Biotium, Hayward, CA, USA). JC-1 was added to cultures for 15 min, and fluorescence was measured with a Gemini XPS microplate reader (Molecular Devices). Red fluorescence (excitation 550 nm, emission 600 nm) indicated intact mitochondria, while green fluorescence (excitation 485 nm, emission 545 nm) corresponded to depolarised mitochondria. Each treatment condition was performed in six technical replicates, and the experiment was independently repeated three times.

 https://doi.org/10.1007/s10616-025-00795-7

Isolation of RNA and amplification of cDNA

143B cells were seeded at a density of 250,000 cells per well in flat-bottomed 6-well plates and incubated at 37 °C for 24 h. Cells were then treated under one of four conditions for the subsequent 48 h: DMSO vehicle control; erastin administered during the final 24 h; continuous treatment with ferrostatin-1 (Fer-1) for 48 h; or pre-treatment with Fer-1 for 24 h followed by co-treatment with erastin and Fer-1 for the remaining 24 h. Total RNA was extracted using the RNeasy Mini Kit (Qiagen), following the manufacturer's protocol and previously established methods (Chang et al. 2022; Schneider et al. 2022). Complementary DNA (cDNA) was synthesised from 1 µg of total RNA using the QuantiTect Reverse Transcription Kit (Qiagen), according to the manufacturer's instructions. The resulting cDNA was subsequently used for quantitative real-time PCR (qRT-PCR) analysis.

Quantitative real-time PCR (qRT-PCR) analyses

Quantitative real-time PCR (qRT-PCR) was conducted on individual cDNA samples using the QuantiFast SYBR Green PCR Kit (Qiagen) on an Applied Biosystems ViiA7 detection system. Gene expression was assessed using commercially validated primers (QuantiTect Primer Assay and KiCqStart Primers; Sigma-Aldrich) targeting components of the System Xc^- antiporter (*SLC7A11*, *SLC3A2*), *GPX4*, *VDAC2*, genes involved in monounsaturated fatty acid (MUFA) and polyunsaturated fatty acid (PUFA) metabolism (*ACSL3*, *LPCAT3*, *ACSL4*), and iron-regulated genes associated with ferroptosis (*TFRC*, *HMOX1*, *FTH1*, *SLC40A1*, *NCOA4*). Expression levels were normalized to the housekeeping gene *HPRT1*. All reactions were performed in triplicate, and relative gene expression was calculated using the $2^{(-\Delta\Delta Ct)}$ method.

Statistical analysis

Statistical analysis was performed using the unpaired, non-parametric Mann–Whitney test (GraphPad Prism version 10.2.3; GraphPad Software, San Diego, CA, USA). A p-value of ≤ 0.05 was considered statistically significant.

Results

ROS and mitochondrial membrane potential are key mediators of erastin-induced death in OS cells

Ferroptosis has recently gained attention as a therapeutic approach for targeting aggressive malignancies. Among the OS cell lines examined, 143B cells demonstrated the most aggressive phenotype, characterized by marked tumorigenicity, predominantly osteolytic lesions, and extensive pulmonary metastasis (Luu et al. 2005). To assess the potential of ferroptosis induction in this context, we treated 143B cells with erastin, a known ferroptosis inducer. Erastin reduced cell viability in a dose-dependent manner (Fig. 1a) and significantly suppressed metabolic activity by approximately 80% ($p < 0.0001$; Fig. 1b). To elucidate the underlying mechanism, we evaluated reactive oxygen species (ROS) levels and mitochondrial membrane potential following erastin exposure. Treatment with erastin led to a greater than fivefold increase in total ROS ($p < 0.0001$) and a tenfold elevation in mitochondrial membrane potential ($p < 0.0001$; Fig. 1c–d). Furthermore, erastin markedly downregulated VDAC2 mRNA expression in 143B cells (Fig. 1e), consistent with its mechanism of action involving inhibition of voltage-dependent anion channels. These findings support the role of erastin in inducing ferroptotic cell death through enhanced oxidative stress and suppression of VDAC2 in aggressive OS cells.

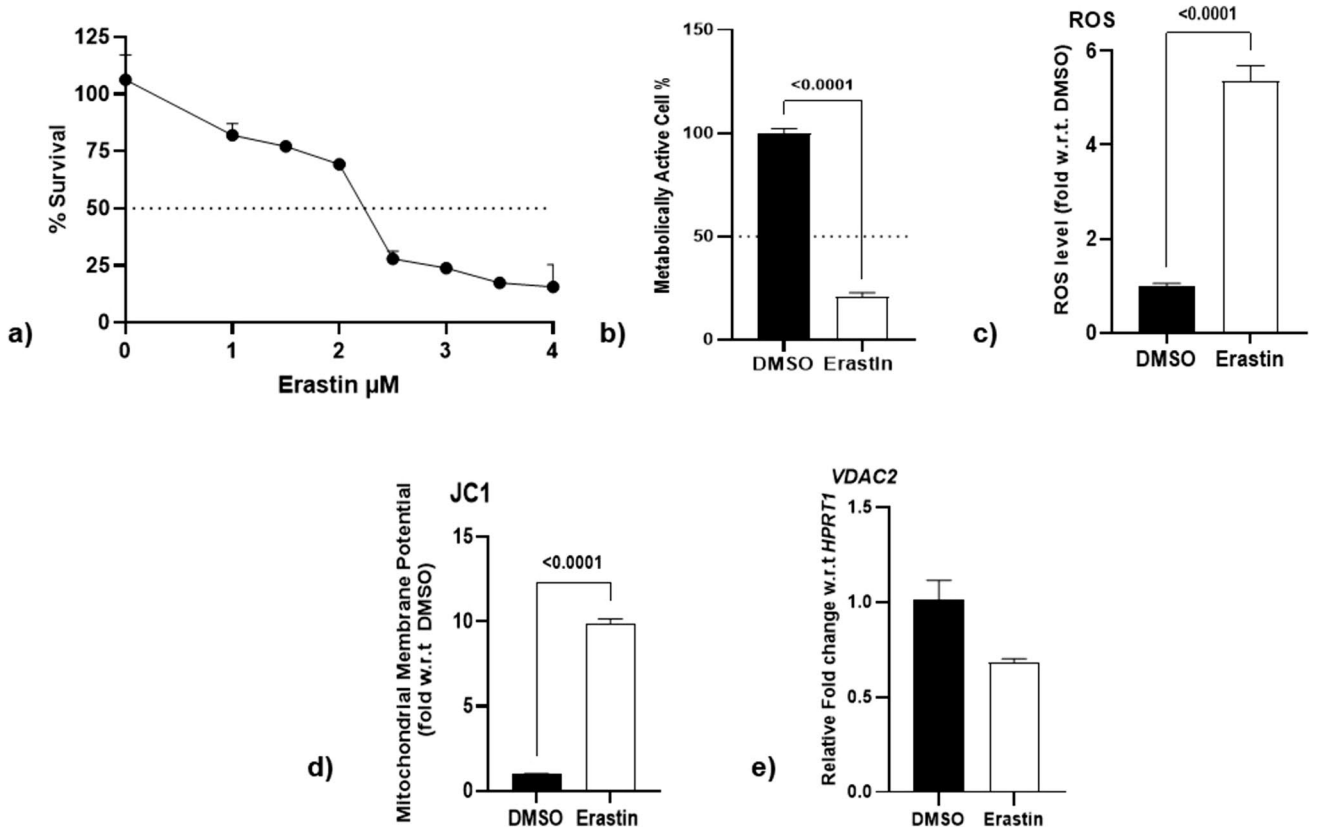

Fig. 1 Erastin negatively impacts metabolic activity, levels of reactive oxygen species (ROS), mitochondrial membrane potential, and mRNA expression of VDAC2 in osteosarcoma cells. **a** Dose–response curves for the effect of erastin treatment. Aggressive OS cells i.e., 143B cells were plated in six replicates in a 96-well plate and treated with 1 µmol/L to 4 µmol/L erastin. Survival was measured after 48 h using MTT assay. Mean ± SD of the replicates normalized to DMSO control are shown. **b**, Effect of ferroptosis inducer (erastin) on the growth of the 143B cells. Cells were plated in six replicates in 96-well plates and treated with 2.25 erastin µmol/L 24 h. Metabolic activity was estimated using MTT assay. **c** Effect of ferroptosis inducer (erastin) on the total ROS of the 143B cells. Cells were plated in six replicates in 96-well plates and treated with 2.25 µmol/L 24 h. Total ROS was estimated using an ROS assay. Fold-change of the replicates normalized to DMSO control. **d** Effect of ferroptosis inducer (erastin) on the mitochondrial membrane potential of the 143B cells. Cells were plated in six replicates in 96-well plates and treated with 2.25 µmol/L 24 h. Mitochondrial membrane potential was estimated using JC1 assay. Fold-change of the replicates normalized to DMSO control. **e** Effect of ferroptosis inducer (erastin) on the *VDAC2* mRNA expression in 143B. 250,000 cells were plated in triplicates in 6-well plates and treated with 2.25 µmol/L 24 h. After 24 h RNA extracted, using 1 µg RNA cDNA synthesized and run qPCR.to detect the mRNA expression of *VDAC2*. Data shown as mean ± SD were analyzed by the Mann Whitney test. p-value ≤ 0.05 is significant

These findings indicate that erastin induces cell death in aggressive OS (143B) cells by elevating total reactive oxygen species, enhancing mitochondrial membrane potential, and downregulating *VDAC2* mRNA expression.

Erastin modulates system Xc^- without affecting enzymes associated with MUFA/PUFA metabolism

Erastin promotes ferroptosis primarily by inhibiting the cystine/glutamate antiporter System Xc^-. To determine its effect on genes associated with this pathway and with glutathione metabolism, we assessed the expression of *SLC3A2*, *SLC7A11*, and *GPX4* in OS cells following erastin treatment. Erastin significantly upregulated *SLC3A2* expression by more than two-fold ($p = 0.0059$) and *SLC7A11* by over five-fold ($p = 0.0005$) (Fig. 2a–b). In contrast, *GPX4* mRNA expression remained unchanged (Fig. 2c). These results suggest that erastin selectively modulates components of

 https://doi.org/10.1007/s10616-025-00795-7

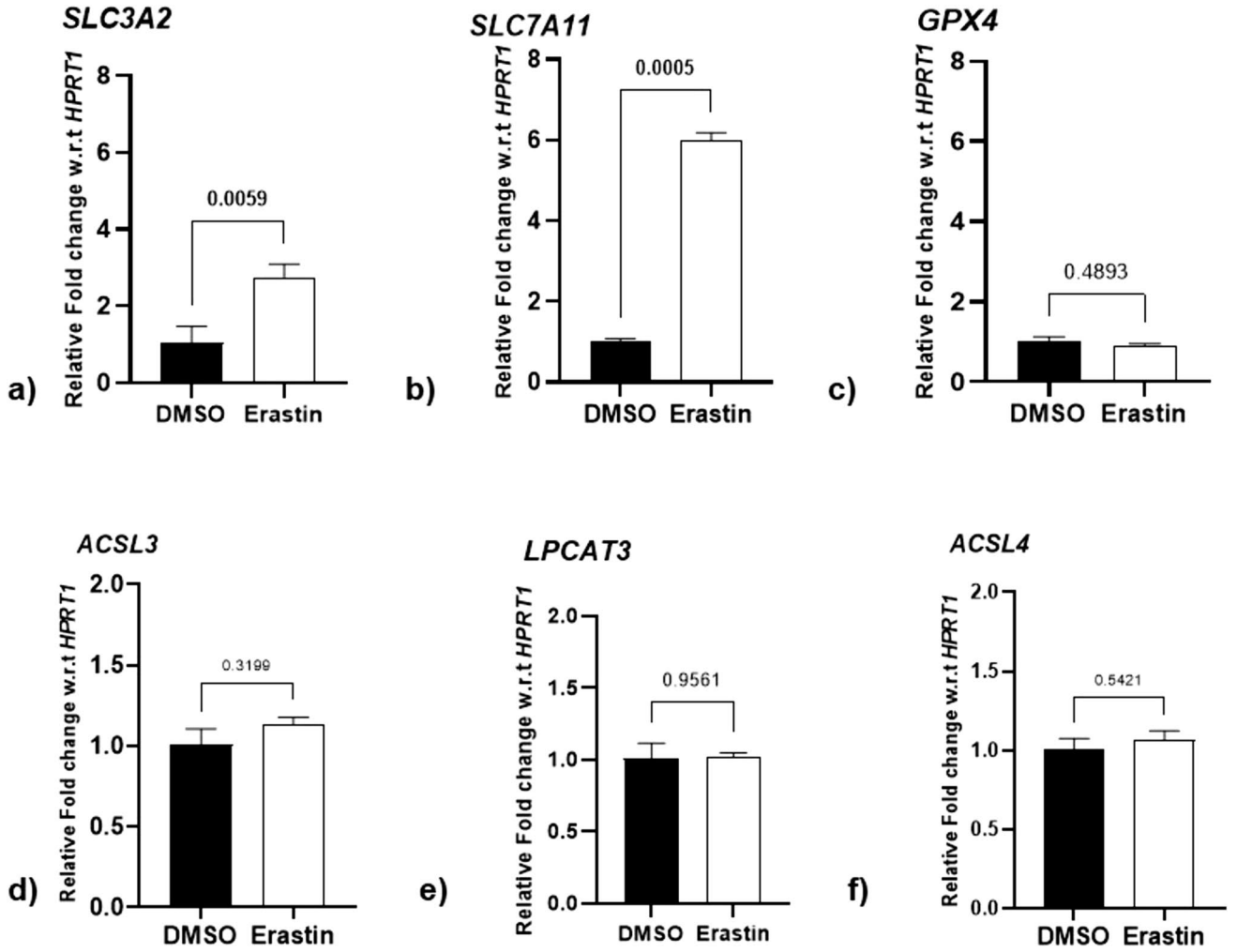

Fig. 2 Erastin alters mRNA expression for System Xc, monounsaturated, and polyunsaturated fatty acids. 250,000 cells were plated in triplicates in 6-well plates and treated with 2.25 µmol/L 24 h following an incubation of 24 h in untreated culture media. After 24 h RNA extracted, using 1 µg RNA cDNA synthesized and run qPCR to detect mRNA expression of: **a** *SLC3A2*; **b** *SLC7A11*; **c** *GPX4*; **d** *ACSL3*; **e** *LPCAT3*; and **f** *ACSL4*. Data shown as mean ± SD were analyzed by the Mann Whitney test. p-value ≤ 0.05 is significant

System Xc^- in OS cells, potentially reflecting a compensatory transcriptional response aimed at mitigating ferroptotic stress.

Accumulating evidence suggests that elevated expression of enzymes involved in polyunsaturated fatty acid (PUFA) metabolism, alongside reduced expression of monounsaturated fatty acid (MUFA) enzymes, contributes to ferroptosis induction in cancer cells. Based on this, we examined the effect of erastin on the expression of key enzymes associated with MUFA and PUFA metabolism in OS cells. Specifically, we assessed *ACSL3* (MUFA-related), *LPCAT3*, and *ACSL4* (both PUFA-related) following erastin treatment. As shown in Fig. 2d–f, erastin did not significantly alter the expression levels of these genes. These results indicate that erastin-induced ferroptosis in OS cells occurs independently of transcriptional changes in MUFA and PUFA metabolism, suggesting alternative mechanisms may underlie its ferroptotic activity in this context.

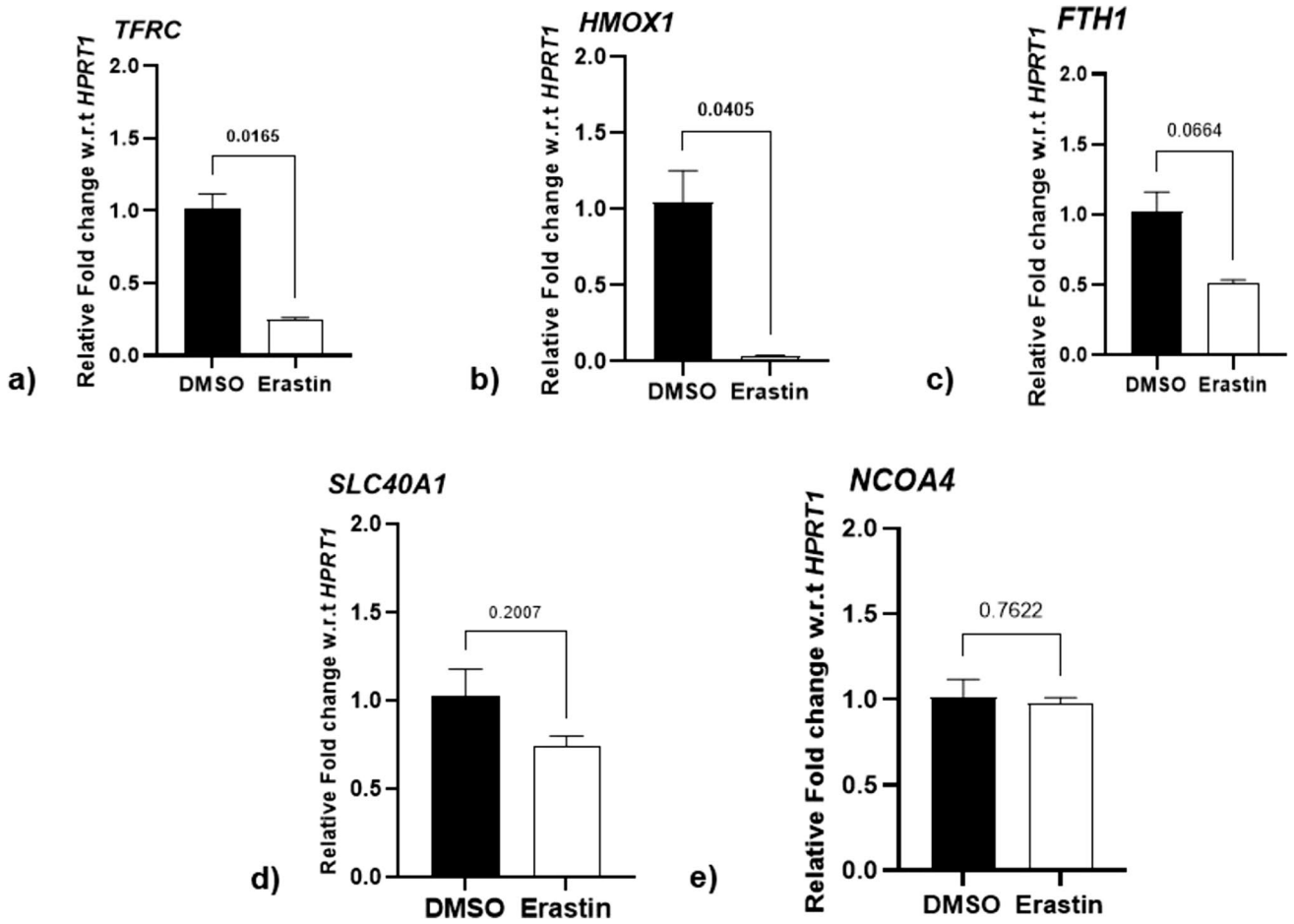

Fig. 3 Erastin inhibits mRNA expression of iron-related genes. 250,000cells were plated in triplicates in 6-well plates and treated with 2.25 µmol/L 24 h. After 24 h RNA extracted, using 1 µg RNA cDNA synthesized and run qPCR to detect mRNA expression of: **a** *TFRC*; **b** *HMOX1*; **c** *FTH1*; **d** *SLC40A1*; and **e** *NCOA4*. Data shown as mean ± SD were analyzed by the Mann Whitney test. p-value ≤ 0.05 is significant

Erastin inhibits mRNA expression of iron-related genes induces ferroptosis in OS cells

Ferroptosis is an iron-dependent form of cell death characterized by dysregulation of iron homeostasis, including activation of ferritinophagy and suppression of genes involved in heme metabolism, iron storage, and transport (Chen et al. 2020). To explore how erastin modulates iron-related pathways in OS cells, we assessed the expression of key genes involved in ferritinophagy, heme degradation, iron uptake, iron storage, and export. Following erastin treatment, OS cells exhibited a marked reduction in the expression of *TFRC* (iron uptake; $p = 0.0165$), *HMOX1* (heme metabolism; $p = 0.0405$), and *FTH1* (ferritin heavy chain; $p = 0.0664$), each showing a decrease of less than 50% relative to control (Fig. 3a–c). In contrast, expression levels of *SLC40A1* (iron export) and *NCOA4* (ferritinophagy) remained unchanged in response to erastin (Fig. 3d–e). These findings suggest that erastin selectively downregulates specific components of intracellular iron handling without modulating ferritinophagy or iron efflux mechanisms in OS cells.

These findings suggest that erastin promotes ferroptosis in OS cells through a mechanism distinct from classical System Xc^- inhibition, potentially by limiting iron uptake. The observed downregulation of *HMOX1* may further indicate a concurrent suppression of anti-ferroptotic responses.

 https://doi.org/10.1007/s10616-025-00795-7

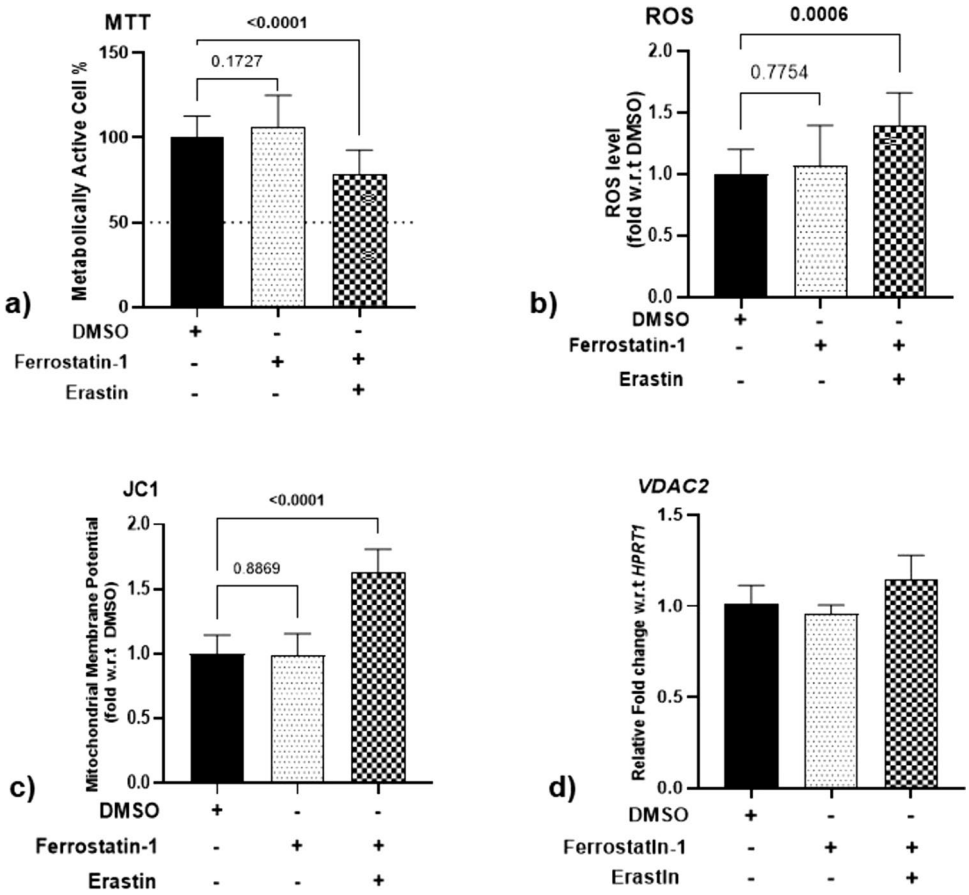

Fig. 4 Impact of ferrostatin-1 on reviving metabolic activity, levels of reactive oxygen species (ROS), mitochondrial membrane potential, and expression of VDAC2 in osteosarcoma cells pre-treated with erastin. Aggressive OS cells i.e., 143B of 10,000 cells were plated in six replicates in a 96-well plate and pre-treated with 2 µmol/L Ferrostatin-1 (Fer-1) 24 h. After 24 h media with a combination of 2 µmol/L Ferrostatin-1 (Fer-1) and 2.25 µmol/L erastin treated for another 24 h. Survival was measured after 48 h using MTT assay. Mean ± SD of the replicates normalized to DMSO control are shown. **a**, Effect of ferroptosis inhibitor (Fer-1) on the growth of the prior erastin-induced 143B cells. Metabolic activity was estimated using MTT assay. **b** Effect of ferroptosis inhibitor (Fer-1) on the total ROS of the prior erastin-induced 143B cells. Total ROS was estimated using an ROS assay. Fold-change of the replicates normalized to DMSO control. **c** Effect of ferroptosis inhibitor (Fer-1) on the total ROS of the prior erastin-induced 143B cells. Mitochondrial membrane potential was estimated using JC1 assay. Fold-change of the replicates normalized to DMSO control. **d** Effect of ferroptosis inhibitor (Fer-1) on the total ROS of the prior erastin-induced 143B cells. 250,000cells were plated in triplicates in 6-well plates and pre-treated with 2 µmol/L Ferrostatin-1 (Fer-1)24 h. After 24 h media was replaced by a combination 2 µmol/L Ferrostatin-1 (Fer-1) and 2.25 µmol/L erastin and incubate for another 24 h. RNA extracted after completion of treatment, using 1 µg RNA cDNA synthesized and run qPCR.to detect the mRNA expression of *VDAC2*. Data shown as mean ± SD were analyzed by the Mann Whitney test. p-value ≤ 0.05 is significant

Effect of ferrostatin-1 on metabolic activity, oxidative stress, mitochondrial function, and VDAC2 mRNA expression in OS cells

To determine whether ferroptosis in OS cells is a reversible or preventable process, we investigated the protective effect of ferrostatin-1 (Fer-1), a known ferroptosis inhibitor, in 143B cells. Cells were pre-treated with Fer-1 for 24 h, followed by an additional 24-h exposure to a combination of erastin and Fer-1. A separate cohort was treated with Fer-1 alone for 48 h to assess its independent effects. As shown in Fig. 4a, treatment with Fer-1 alone had no significant impact on metabolic activity. However, pre-treatment with Fer-1 partially attenuated the cytotoxic effect of erastin, resulting in only a 20% reduction in metabolic activity ($p < 0.0001$), compared to the 80% reduction observed with erastin alone (Fig. 1b).

We next examined the influence of Fer-1 on reactive oxygen species (ROS) generation. As previously shown (Fig. 1c), erastin treatment induced a greater than fivefold increase in total ROS. While co-treatment with Fer-1 significantly reduced ROS accumulation in erastin-exposed cells, ROS levels remained elevated—more than 50% above control ($p < 0.0006$; Fig. 4b). Fer-1 alone did not alter ROS levels, indicating it does not provoke oxidative stress under basal conditions.

We further assessed mitochondrial membrane potential, a hallmark of ferroptotic stress. Erastin treatment alone resulted in a tenfold increase in mitochondrial membrane potential (Fig. 1d). In contrast, Fer-1 co-treatment reduced this effect, producing only a twofold increase in erastin-treated cells ($p < 0.0001$; Fig. 4c). Notably, Fer-1 alone had no measurable effect on mitochondrial membrane potential in OS cells.

Finally, we investigated whether Fer-1 could modulate the expression of *VDAC2*, a known erastin target. As shown in Fig. 4d, Fer-1 treatment alone had no impact on *VDAC2* expression. However, in the context of erastin exposure, Fer-1 partially restored *VDAC2* expression levels, suggesting a mitigating effect on erastin-induced transcriptional suppression. These findings collectively indicate that Fer-1 exerts a partial protective effect against erastin-induced ferroptosis in OS cells by modulating oxidative stress, mitochondrial function, and *VDAC2* expression.

These findings suggest that Fer-1 confers partial protection against erastin-induced ferroptosis in aggressive OS cells. This protective effect appears to be mediated through attenuation of oxidative stress, as evidenced by a reduction in total reactive oxygen species (ROS) levels, and partial restoration of mitochondrial membrane potential. Additionally, Fer-1 modestly increased *VDAC2* mRNA expression in the presence of erastin, implicating this mitochondrial channel as a potential target in the ferroptotic pathway. Together, these results indicate that Fer-1 mitigates ferroptotic damage by modulating key molecular and functional markers associated with ferroptosis in OS cells.

Ferrostatin-1 pre-treatment enhances System Xc^- and lipid metabolic enzymes gene expression in erastin-induced OS cells

Figures 2a–f demonstrates that erastin-induced ferroptosis in 143B OS cells does not result in suppression of SLC3A2 or SLC7A11, the two essential components of the cystine/glutamate antiporter System Xc^-. On the contrary, erastin treatment significantly increased the expression of both genes, suggesting a compensatory upregulation in response to ferroptotic stress. This paradoxical induction of *SLC3A2* and *SLC7A11* may reflect a cellular feedback mechanism aimed at restoring redox balance and resisting ferroptotic cell death in aggressive OS cells. Furthermore, erastin had no observable effect on the expression of GPX4, a central antioxidant enzyme that detoxifies lipid peroxides, nor on the expression of key enzymes involved in lipid metabolism, including ACSL3 (monounsaturated fatty acid metabolism), LPCAT3, and ACSL4 (polyunsaturated fatty acid metabolism).

To explore whether this adaptive gene expression profile could be altered by ferroptosis inhibition, we examined the effects of Fer-1 on these regulatory pathways. As shown in Fig. 5a–b, Fer-1 alone did not significantly affect *SLC3A2* or *SLC7A11* expression. However, pre-treatment with Fer-1 for 24 h prior to combined Fer-1 and erastin exposure led to a marked eightfold increase in the mRNA levels of both genes, suggesting that Fer-1 may further enhance System Xc^- activity under ferroptotic conditions. This amplification may represent a protective cellular response to oxidative stress, potentially contributing to resistance mechanisms.

Consistent with earlier findings, *GPX4* expression remained unchanged across all treatment conditions, including Fer-1 alone and Fer-1 pre-treatment followed by erastin exposure (Fig. 5c), indicating that its transcription is not significantly influenced by ferroptosis or its inhibition in this model. Similarly, Fer-1 alone had no impact on the expression of *ACSL3*, *LPCAT3*, or *ACSL4*. However, pre-treatment with Fer-1 followed by co-treatment with erastin significantly upregulated the expression of these lipid-metabolizing enzymes by approximately twofold (Fig. 5d–f).

These findings collectively suggest that Fer-1, in the context of ferroptotic stress, can modulate transcriptional responses related to cystine import and lipid metabolism. This dual regulatory effect may contribute to an adaptive

 https://doi.org/10.1007/s10616-025-00795-7

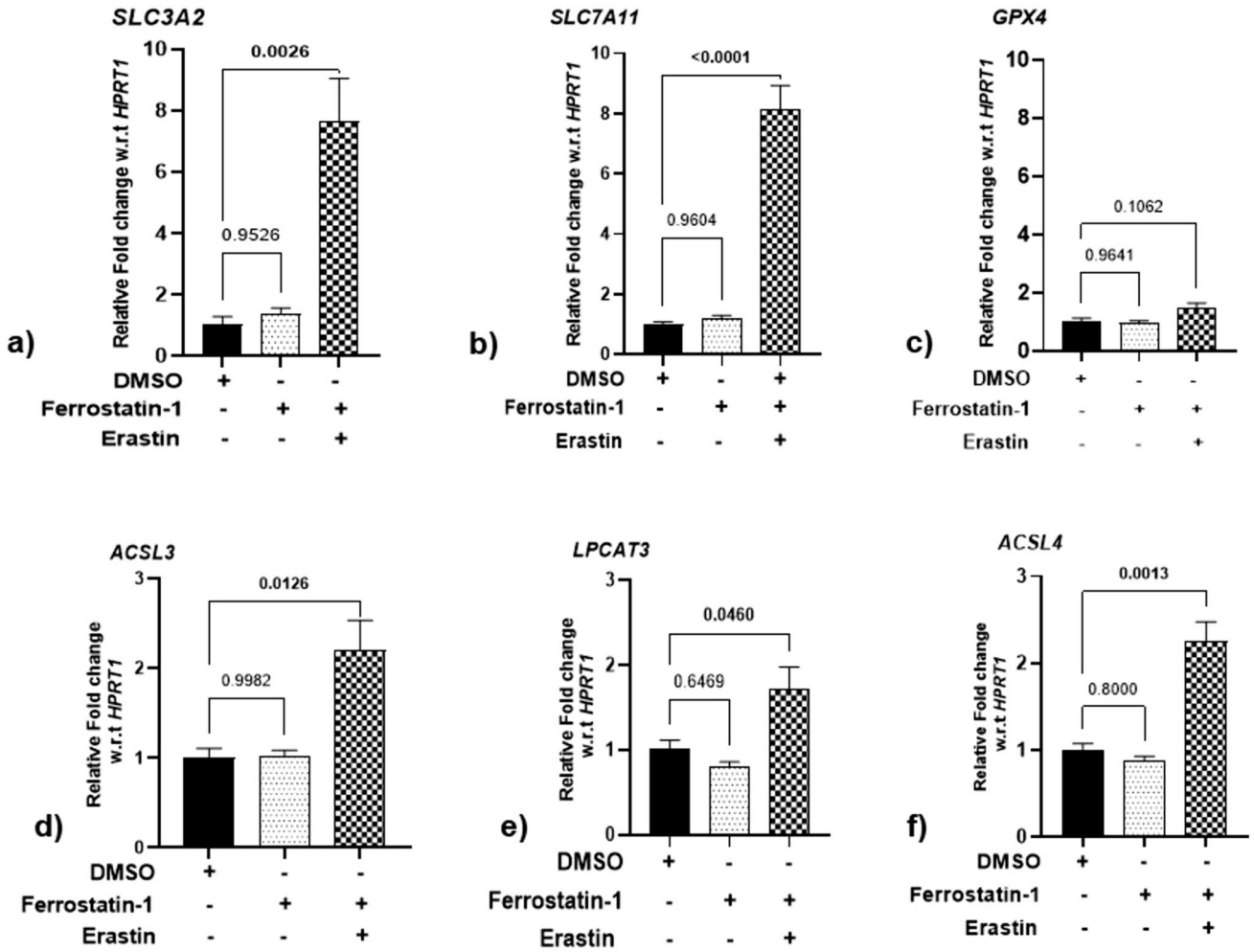

Fig. 5 Effect of ferrostatin-1 on the mRNA expression of System Xc, monounsaturated, and polyunsaturated fatty acids in osteosarcoma cells pretreated with erastin. Aggressive OS cells i.e., 143B of 250,000 cells were plated in triplicates in 6-well plates and pre-treated with 2 µmol/L Fer-1 for 24 h. After 24 h, media was replaced by a combination of 2 µmol/L Fer-1 and 2.25 µmol/L erastin and incubated for another 24 h RNA extracted after completion of treatment, using 1 µg RNA cDNA synthesized and run qPCR.to detect the mRNA expression of: **a** *SLC3A2*; **b** *SLC7A11*; **c** *GPX4*; **d** *ACSL3*; **e** *LPCAT3*; and **f** *ACSL4*. Data shown as mean ± SD were analyzed by the Mann Whitney test. p-value ≤ 0.05 is significant

program that enhances cellular survival under ferroptotic conditions, potentially diminishing the efficacy of ferroptosis-inducing agents in aggressive OS cells.

Ferrostatin-1 modulates iron homeostasis genes in erastin-induced OS cells

As previously demonstrated (Fig. 3a–c), erastin promotes ferroptosis in OS cells through downregulation of genes involved in iron uptake (TFRC), heme metabolism (HMOX1), and iron storage (FTH1). To further assess whether ferrostatin-1 (Fer-1) can counteract this effect, we investigated whether pre-treatment with Fer-1 prior to combined erastin and Fer-1 exposure modulates the expression of iron-regulatory genes. Specifically, we examined genes involved in iron uptake, heme degradation, ferritin synthesis, iron export, and ferritinophagy.

As shown in Fig. 6a–e, treatment with Fer-1 alone had no significant effect on the expression of *TFRC*, *HMOX1*, *FTH1*, *SLC40A1* (iron export), or *NCOA4* (ferritinophagy). Interestingly, Fer-1 pre-treatment followed by co-treatment with erastin produced only modest reductions in *TFRC* ($p = 0.0389$) and *HMOX1* ($p = 0.0319$) expression

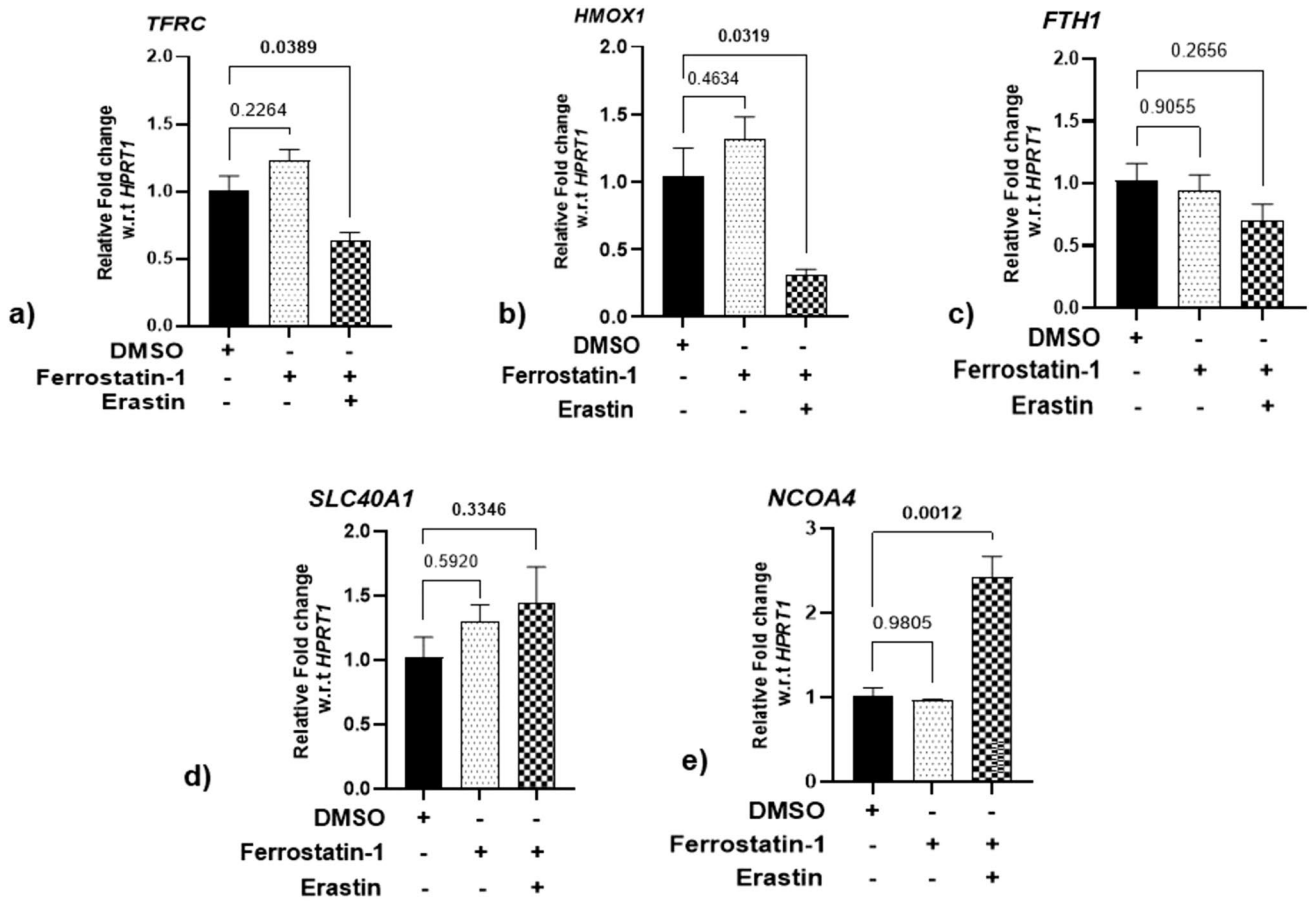

Fig. 6 Effect of ferrostatin-1 on the mRNA expression of iron-related genes in osteosarcoma cells pretreated with erastin. Aggressive OS cells i.e., 143B of 250,000 cells were plated in triplicates in 6-well plates and pre-treated with 2 µmol/L Fer-1 for 24 h. After 24 h, media was replaced by a combination of 2 µmol/L Fer-1 and 2.25 µmol/L erastin and incubated for another 24 h RNA extracted after completion of treatment, using 1 µg RNA cDNA synthesized and run qPCR.to detect the mRNA expression of: **a** *TFRC*; **b** *HMOX1*; **c** *FTH1*; **d** *SLC40A1*; and **e** *NCOA4*. Data shown as mean ± SD were analyzed by the Whitney test. p-value ≤ 0.05 is significant

levels, suggesting limited suppression of iron uptake and heme catabolism under these conditions. Notably, this treatment significantly upregulated NCOA4 expression ($p = 0.0012$), a key mediator of ferritinophagy, indicating a potential shift toward enhanced ferritin degradation and intracellular iron mobilization.

These findings suggest that Fer-1 confers partial protection against ferroptosis in OS cells by attenuating iron influx and heme metabolism, while paradoxically increasing *NCOA4* expression potentially promoting ferritinophagy. The reduction of *HMOX1*, typically involved in iron release from heme, may reflect a compensatory, anti-ferroptotic response. Overall, the data highlights a complex regulatory interplay wherein Fer-1 may both suppress and facilitate ferroptotic processes depending on the balance of iron regulatory mechanisms in the cellular context.

Discussion

In this study demonstrates that Erastin treatment significantly reduced cell viability and metabolic activity in 143B cells in a dose-dependent manner and induced ferroptosis, as evidenced by elevated reactive oxygen species (ROS), increased mitochondrial membrane potential, and downregulation of *VDAC2*. Despite these effects, erastin upregulated *SLC3A2* and *SLC7A11* (System Xc^- components), suggesting a compensatory transcriptional

 https://doi.org/10.1007/s10616-025-00795-7

response, while leaving *GPX4*, *ACSL3*, *LPCAT3*, and *ACSL4* expression unchanged. Additionally, erastin suppressed genes involved iron homeostasis, including *TFRC*, *HMOX1*, and *FTH1*, without affecting *SLC40A1* or *NCOA4*. Pre-treatment with Fer-1 partially attenuated erastin-induced reductions in metabolic activity, ROS production, and mitochondrial membrane hyperpolarization, and modestly restored *VDAC2* mRNA expression. While Fer-1 alone did not alter the expression of System Xc^-, MUFA/PUFA, or iron-related genes, its pre-treatment before erastin exposure significantly amplified *SLC3A2*, *SLC7A11*, *ACSL3*, *LPCAT3*, and *ACSL4* expression. Furthermore, Fer-1 pre-treatment resulted in a modest decrease in *TFRC* and *HMOX1*, and a significant increase in *NCOA4* expression, suggesting selective modulation of ferritinophagy and iron homeostasis under ferroptotic stress. Collectively, these findings indicate that erastin induces ferroptosis in OS cells through mitochondrial dysfunction and disrupted iron metabolism, while Fer-1 exerts partial protective effects and may contribute to transcriptional adaptations that influence ferroptosis sensitivity (Fig. 7).

Many aggressive cancer cells provide indirect protection against Erastin by inhibiting *GPX4* via GSH depletion (Yang et al. 2014). *GPX4* has recently been identified as a key regulator of ferroptosis (14), an iron-dependent non-apoptotic mechanism of cell death (Galluzzi et al. 2015). Interestingly, Reina et al. found that erastin can promote transcriptional activation of *SLC7A11* (Reina and Pinto 2017). Overexpression of *SLC7A11* via gene transfection reduced erastin-induced cell death, but inhibition of *SLC7A11* expression boosted erastin's anticancer efficacy (Dixon et al. 2012). Erastin inhibits system X_C, which indirectly reduces cystine uptake in cells. Erastin's inhibition of system X_C suggests that, in addition to affecting VDAC permeability, it can activate the ferroptosis pathway by targeting system X_C (Zhang et al. 2018). Consistent with this, we found that erastin treatment reduced aggressive OS cell growth while increasing the transcriptional

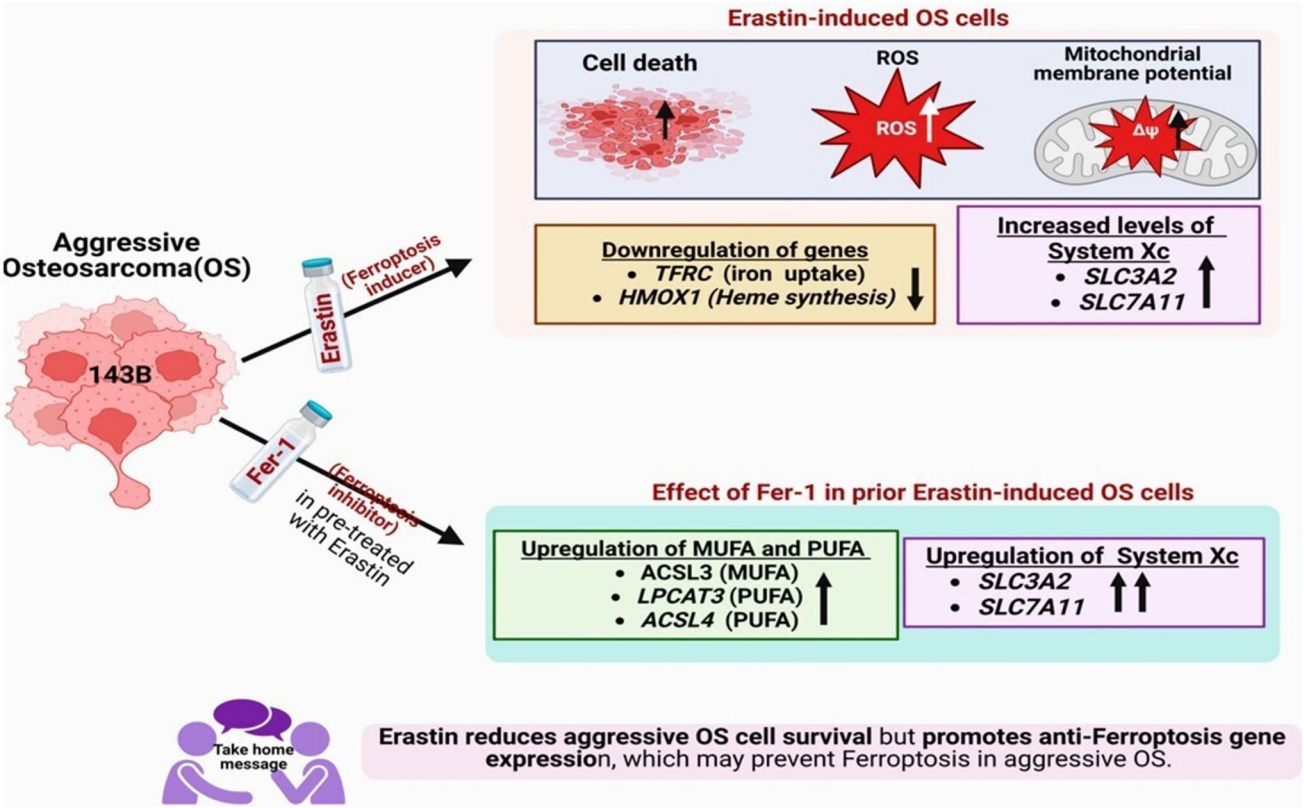

Fig. 7 Schematic representation of erastin and ferrostatin-1 (Fer-1) in aggressive OS cells. Treatment with erastin may induce ferroptosis by sensitizing the survival of aggressive OS cells by modulation of total ROS and mitochondrial membrane potential. In aggressive OS cells, treatment with Fer-1 before erastin treatment highlights the phenomena of activation of specific gene expression associated with anti-ferroptosis, which could eventually result in the emergence of resistance to ferroptosis

activity of *SLC7A11* and *SLC3A2*, indicating compensatory transcriptional upregulation. In contrast, erastin treatment does not alter the expression level of *GPX4*. Interestingly, we also found that Fer-1 can boost the overexpression of *SLC7A11* and *SLC3A2* while having no effect on *GPX4* expression in erastin-induced OS cells, implying that it could develop anti-ferroptotic activity.

HMOX1 performs dual functions in ferroptosis induction. On the one hand, erastin stimulates the expression of *HMOX1*, which may increase ferroptosis in HT1080 fibrosarcoma cells. They also demonstrated that *HMOX1* deletion suppresses, whereas *HMOX1* overexpression increases ferroptotic cancer cell death mediated by erastin (Kwon et al. 2015). In contrast to this study, we found that erastin-induced OS cells reduce *HMOX1* expression, and Fer-1 pre-treatment in erastin-induced OS cells likewise inhibits *HMOX1* expression, indicating that it may have the potential to acquire resistance to ferroptosis.

The expression level of *TFRC* is reduced in renal papillary cell carcinoma, lung adenocarcinoma, paraganglioma, prostate cancer, and thyroid cancer, and the prognosis of patients with high TFRC expression is relatively poor, implying that *TFRC* expression level is closely related to the prognosis of different cancers (Karthiya and Khandelia 2020). Interestingly, we found that erastin-induced OS cells suppress the production of *TFRC* and *FTH1*, which is specific to ferroptosis.

In contrast, erastin suppressed *FTH1* (ferritin heavy chain), potentially destabilizing ferritin complexes and increasing the labile iron pool. *NCOA4*, which regulates ferritinophagy, remained unchanged, suggesting preserved intracellular iron mobilization. This expression profile points to a shift from iron uptake to redistribution from internal stores as the predominant mechanism sustaining ferroptosis in this setting (Yan et al. 2021; Gao et al. 2019).

These observations align with emerging evidence that ferroptosis can proceed independently of transferrin-mediated uptake when intracellular iron sources, such as ferritin degradation, are activated (Dixon et al. 2012; Mancias et al. 2015; Guggisberg et al. 2022). Our results reinforce this model, highlighting *FTH1* suppression and stable *NCOA4* expression as key features of iron homeostasis disruption under ferroptotic stress. The observed *TFRC* downregulation may reflect a compensatory response to elevated cytosolic iron, rather than a barrier to ferroptosis initiation.

ACSL4 has been reported to be overexpressed in several cancer types (Wu et al. 2013, 2015; Sánchez-Martínez et al. 2017; Xia et al. 2017). It enriches cellular membranes with long polyunsaturated ω-6 fatty acids and helps produce lipid peroxidation. Furthermore, in comparison to ferroptosis-sensitive cancer cells, the expression of *ACSL4* was significantly downregulated in ferroptosis-resistant cancer cells (Yuan et al. 2016). As a result, boosting *ACSL4* promotes tumor growth and proliferation while also increasing ferroptosis susceptibility. In contrast, our study observed no change in the expression levels of *ACSL4* or *LPCAT3* in erastin-induced OS cells. Interestingly, Fer-1 treatment in earlier erastin-induced OS cells increases the expression of *ACSL4* and *LPCAT3*, indicating anti-ferroptotic activation.

The results of this study suggest that ferroptosis induction, particularly through agents such as erastin, represents a promising therapeutic avenue for the treatment of aggressive and treatment-resistant OS cells. By targeting mitochondrial dysfunction and disrupting iron homeostasis, erastin effectively compromises OS cell viability. Furthermore, the observation that ferroptosis inhibition via ferrostatin-1 leads to compensatory upregulation of *System* Xc^- and lipid metabolism genes highlights potential mechanisms of resistance. This underscores the clinical potential of combination strategies using ferroptosis inducers alongside inhibitors of adaptive antioxidants or lipid regulatory pathways to enhance treatment efficacy and overcome resistance. Such approaches may be particularly valuable in relapsed or refractory OS cases, where conventional therapies often fail.

While the findings presented here offer novel insights into the molecular mechanisms underlying ferroptosis in OS, the study has several limitations. All experiments were conducted in vitro using a single cell line (143B), which may not fully represent the heterogeneity of OS in patients. Further investigation in additional OS models and in vivo systems is essential to validate these findings and assess therapeutic relevance. Additionally, although mRNA expressions of key genes were examined, corresponding protein expression and functional validation were not comprehensively evaluated. This limits the ability to confirm direct mechanistic effects. Finally, the safety

profile and selectivity of ferroptosis induction in malignant versus normal osteogenic cells remain unknown, and future studies should address these issues to inform potential clinical translation.

Despite these limitations, our findings offer important mechanistic insight into ferroptosis in OS and lay the groundwork for future therapeutic development. Understanding how ferroptosis is influenced by cystine transport, lipid metabolism, and heme-related gene regulation may inform novel therapeutic strategies, particularly for patients with advanced or treatment-resistant OS cells. These results support the further exploration of ferroptosis as a targeted vulnerability in OS.

Supplementary Information The online version contains supplementary material available at https://doi.org/10.1007/s10616-025-00795-7.

Author contributions GDB, MC, KS, SA, MCK, and MKS designed and performed the experiments. GDB, MC, KS, SA and MKS analyzed all the data and results. GDB, MKS and SC original draft, review, and editing of the manuscript. MCK provided resources and supervision. All authors have reviewed and agreed to the published version of the manuscript.

Funding This work was supported by funding from the Discovery Eye Foundation, an unrestricted grant from the Research to Prevent Blindness Foundation and NEI R01 EY027363 (MCK). These funding sources had no role in the direction of this study or its submission for publication. We acknowledge the support of the Institute for Clinical and Translational Science (ICTS) at University of California Irvine (ULI TR001414/TR/NCATS). GDB is a recipient of the 2023 UCI Undergraduate Research Opportunities Research Program. M.K.S is the recipients of the Arnold and Mabel Beckman Retinal Degeneration Fellow.

Data availability No datasets were generated or analysed during the current study.

Declarations

Conflict of interest The authors declare no competing interests.

References

Bernthal NM, Federman N, Eilber FR, Nelson SD, Eckardt JJ, Eilber FC, Tap WD (2012) Long-term results (>25 years) of a randomized, prospective clinical trial evaluating chemotherapy in patients with high-grade, operable osteosarcoma. Cancer 118:5888–5893

Brack E, Wachtel M, Wolf A, Kaech A, Ziegler U, Schäfer BW (2020) Fenretinide induces a new form of dynamin-dependent cell death in pediatric sarcoma. Cell Death Differ 27:2500–2516

Chang S, Singh L, Thaker K, Abedi S, Singh MK, Patel TH, Chwa M, Atilano SR, Udar N, Bota D et al (2022) Altered retrograde signaling patterns in breast cancer cells cybrids with H and J mitochondrial DNA haplogroups. Int J Mol Sci 23:6687

Chen X, Yu C, Kang R, Tang D (2020) Iron metabolism in ferroptosis. Front Cell Dev Biol 8:590226

Codenotti S, Poli M, Asperti M, Zizioli D, Marampon F, Fanzani A (2018) Cell growth potential drives ferroptosis susceptibility in rhabdomyosarcoma and myoblast cell lines. J Cancer Res Clin Oncol 144:1717–1730

Collins M, Wilhelm M, Conyers R, Herschtal A, Whelan J, Bielack S, Kager L, Kühne T, Sydes M, Gelderblom H et al (2013) Benefits and adverse events in younger versus older patients receiving neoadjuvant chemotherapy for osteosarcoma: findings from a meta-analysis. J Clin Oncol 31:2303–2312

Dixon SJ, Lemberg KM, Lamprecht MR, Skouta R, Zaitsev EM, Gleason CE, Patel DN, Bauer AJ, Cantley AM, Yang WS et al (2012) Ferroptosis: an iron-dependent form of nonapoptotic cell death. Cell 149:1060–1072

Galadari S, Rahman A, Pallichankandy S, Thayyullathil F (2017) Reactive oxygen species and cancer paradox: to promote or to suppress? Free Radic Biol Med 104:144–164

Galluzzi L, Bravo-San Pedro JM, Vitale I, Aaronson SA, Abrams JM, Adam D, Alnemri ES, Altucci L, Andrews D, Annicchiarico-Petruzzelli M et al (2015) Essential versus accessory aspects of cell death: recommendations of the NCCD 2015. Cell Death Differ 22:58–73

Gao M, Yi J, Zhu J, Minikes AM, Monian P, Thompson CB, Jiang X (2019) Role of mitochondria in ferroptosis. Mol Cell 73:354-363.e353

Guggisberg CA, Kim J, Lee J, Chen X, Ryu MS (2022) NCOA4 regulates iron recycling and responds to hepcidin activity and lipopolysaccharide in macrophages. Antioxidants (Basel) 11:1926

Hedrick E, Mohankumar K, Lacey A, Safe S (2019) Inhibition of NR4A1 promotes ROS accumulation and IL24-dependent growth arrest in rhabdomyosarcoma. Mol Cancer Res 17:2221–2232
Karthiya R, Khandelia P (2020) m6A RNA methylation: ramifications for gene expression and human health. Mol Biotechnol 62:467–484
Kwon MY, Park E, Lee SJ, Chung SW (2015) Heme oxygenase-1 accelerates erastin-induced ferroptotic cell death. Oncotarget 6:24393–24403
Lei Y, Junxin C, Yongcan H, Xiaoguang L, Binsheng Y (2020) Role of microRNAs in the crosstalk between osteosarcoma cells and the tumour microenvironment. J Bone Oncol 25:100322
Liu M, Fan Y, Li D, Han B, Meng Y, Chen F, Liu T, Song Z, Han Y, Huang L et al (2021) Ferroptosis inducer erastin sensitizes NSCLC cells to celastrol through activation of the ROS-mitochondrial fission-mitophagy axis. Mol Oncol 15:2084–2105
Luu HH, Kang Q, Park JK, Si W, Luo Q, Jiang W, Yin H, Montag AG, Simon MA, Peabody TD et al (2005) An orthotopic model of human osteosarcoma growth and spontaneous pulmonary metastasis. Clin Exp Metastasis 22:319–329
Mancias JD, Pontano Vaites L, Nissim S, Biancur DE, Kim AJ, Wang X, Liu Y, Goessling W, Kimmelman AC, Harper JW (2015) Ferritinophagy via NCOA4 is required for erythropoiesis and is regulated by iron dependent HERC2-mediated proteolysis. Elife 4:e10308
Meyers PA, Healey JH, Chou AJ, Wexler LH, Merola PR, Morris CD, Laquaglia MP, Kellick MG, Abramson SJ, Gorlick R (2011) Addition of pamidronate to chemotherapy for the treatment of osteosarcoma. Cancer 117:1736–1744
Mirabello L, Troisi RJ, Savage SA (2009) Osteosarcoma incidence and survival rates from 1973 to 2004: data from the surveillance, epidemiology, and end results program. Cancer 115:1531–1543
Ottaviani G, Jaffe N (2009) The epidemiology of osteosarcoma. Cancer Treat Res 152:3–13
Reina S, De Pinto V (2017) Anti-cancer compounds targeted to VDAC: potential and perspectives. Curr Med Chem 24:4447–4469
Sadykova LR, Ntekim AI, Muyangwa-Semenova M, Rutland CS, Jeyapalan JN, Blatt N, Rizvanov AA (2020) Epidemiology and risk factors of osteosarcoma. Cancer Invest 38:259–269
Sánchez-Martínez R, Cruz-Gil S, García-Álvarez MS, Reglero G, Ramírez de Molina A (2017) Complementary ACSL isoforms contribute to a non-Warburg advantageous energetic status characterizing invasive colon cancer cells. Sci Rep 7:11143
Schneider K, Chwa M, Atilano SR, Nashine S, Udar N, Boyer DS, Jazwinski SM, Miceli MV, Nesburn AB, Kuppermann BD et al (2022) Differential modulation of cancer-related genes by mitochondrial DNA haplogroups and the STING DNA sensing system. FASEB Bioadv 4:675–689
Schott C, Graab U, Cuvelier N, Hahn H, Fulda S (2015) Oncogenic RAS mutants confer resistance of RMS13 rhabdomyosarcoma cells to oxidative stress-induced ferroptotic cell death. Front Oncol 5:131
Torii S, Shintoku R, Kubota C, Yaegashi M, Torii R, Sasaki M, Suzuki T, Mori M, Yoshimoto Y, Takeuchi T et al (2016) An essential role for functional lysosomes in ferroptosis of cancer cells. Biochem J 473:769–777
Ursini F, Bosello Travain V, Cozza G, Miotto G, Roveri A, Toppo S, Maiorino M (2022) A white paper on phospholipid hydroperoxide glutathione peroxidase (GPx4) forty years later. Free Radic Biol Med 188:117–133
Wang H (2020) MicroRNAs and apoptosis in colorectal cancer. Int J Mol Sci 21:5353
Wu X, Li Y, Wang J, Wen X, Marcus MT, Daniels G, Zhang DY, Ye F, Wang LH, Du X et al (2013) Long chain fatty Acyl-CoA synthetase 4 is a biomarker for and mediator of hormone resistance in human breast cancer. PLoS ONE 8(10):e77060
Wu X, Deng F, Li Y, Daniels G, Du X, Ren Q, Wang J, Wang LH, Yang Y, Zhang V et al (2015) ACSL4 promotes prostate cancer growth, invasion and hormonal resistance. Oncotarget 6:44849–44863
Xia H, Lee KW, Chen J, Kong SN, Sekar K, Deivasigamani A, Seshachalam VP, Goh BKP, Ooi LL, Hui KM (2017) Simultaneous silencing of ACSL4 and induction of GADD45B in hepatocellular carcinoma cells amplifies the synergistic therapeutic effect of aspirin and sorafenib. Cell Death Discov 3:17058
Xu T, Ding W, Ji X, Ao X, Liu Y, Yu W, Wang J (2019) Molecular mechanisms of ferroptosis and its role in cancer therapy. J Cell Mol Med 23:4900–4912
Yan HF, Zou T, Tuo QZ, Xu S, Li H, Belaidi AA, Lei P (2021) Ferroptosis: mechanisms and links with diseases. Signal Transduct Target Ther 6:49
Yang WS, SriRamaratnam R, Welsch ME, Shimada K, Skouta R, Viswanathan VS, Cheah JH, Clemons PA, Shamji AF, Clish CB et al (2014) Regulation of ferroptotic cancer cell death by GPX4. Cell 156:317–331
Yang Y, Luo M, Zhang K, Zhang J, Gao T, Connell DO, Yao F, Mu C, Cai B, Shang Y et al (2020) Nedd4 ubiquitylates VDAC2/3 to suppress erastin-induced ferroptosis in melanoma. Nat Commun 11:433
Yuan H, Li X, Zhang X, Kang R, Tang D (2016) Identification of ACSL4 as a biomarker and contributor of ferroptosis. Biochem Biophys Res Commun 478:1338–1343
Zhang Y, Yang J, Zhao N, Wang C, Kamar S, Zhou Y, He Z, Yang J, Sun B, Shi X et al (2018) Progress in the chemotherapeutic treatment of osteosarcoma. Oncol Lett 16:6228–6237
Zhang W, Liu Y, Liao Y, Zhu C, Zou Z (2024) GPX4, ferroptosis, and diseases. Biomed Pharmaco 174:116512

Zilka O, Shah R, Li B, Friedmann Angeli JP, Griesser M, Conrad M, Pratt DA (2017) On the mechanism of cytoprotection by ferrostatin-1 and liproxstatin-1 and the role of lipid peroxidation in ferroptotic cell death. ACS Cent Sci 3:232–243

Authors and Affiliations

Gordon Daniel Burns[1] · Kevin Schneider[1] · Shari Atilano[1] · Marilyn Chwa[1] · Steven Chang[1] · M. Cristina Kenney[1,2] · Mithalesh Kumar Singh[1,3]

✉ Mithalesh Kumar Singh
mithalesh.aiims@gmail.com

Gordon Daniel Burns
burnsgd@uci.edu

Kevin Schneider
kschneid@uci.edu

Shari Atilano
shariatilano@yahoo.com

Marilyn Chwa
mchwa57@yahoo.com

Steven Chang
sychang2@uci.edu

M. Cristina Kenney
mkenney@hs.uci.edu

[1] Department of Ophthalmology, Gavin Herbert Eye Institute, University of California Irvine, Irvine, CA 92697, USA

[2] Department of Pathology and Laboratory Medicine, University of California Irvine, Irvine, CA 92697, USA

[3] Department of Ophthalmology, UT Southwestern Medical Center, Dallas, TX, USA